

# Calculated Structural and Electronic Interactions of the nano dye molecule $\text{Ru}(\text{4,4} - \text{COOH} - 2,2 - \text{bpy})_2(\text{NCS})_2(\text{N3})$ with a iodide/triiodide redox shuttle

E. Shomali, I. Abdolhosseini Sarsari, S. Javad Hashemifar, and M. Alaei  
*Department of Physics, Isfahan University of Technology,  
 Isfahan, 84156-83111, Iran*

(Dated: November 9, 2018)

In this paper, dye sensitized solar cell based on nano dye molecule N3 are investigated by using density functional computations. The main focus is on the N3 dye molecule and corresponding complexes formed at the interface between electrolyte and dye, during the regeneration process. The optimized geometry and electronic structure of the molecule and complexes are calculated by using the pseudopotential as well as full-potential techniques. The absorption spectra of metalliferous dye molecule, N3, and its complexes are computed in the framework of time dependent density functional theory. We determine the reaction path of dye regeneration by Nudged Elastic Band (NEB) method. IR spectrum of the N3 dye molecule were also calculated. We found that complexes of N3 dye molecule and transition states formed in reactions, are magnetic.

## I. INTRODUCTION

The world energy demand is increasing while the main energy resource, fossil fuels, are limited. Moreover, these conventional energy resources are usually accompanied with various kinds of environmental pollutions. Therefore, renewable and clean energy sources, including wind, geothermal, marine and tides, biomass, and solar energy [1] are strongly desired. Solar photovoltaic is likely the leading renewable energy technology which is expected to provide an energy share of about 16% in 2050 based on Technology Roadmap Solar Photovoltaic Energy, 2014. First generation solar cells are based on crystalline silicon that are stable and have a high efficiency but their construction is costly. Second generation solar cells, which employ non-crystalline silicon, have lower efficiency and cost than the first generation. Third generation solar cells are based on organic materials, consisting of dye sensitized solar cells, polymer solar cells, and liquid-crystal solar cells [2–4]. Although dye sensitized solar cells have low efficiency (almost 11.1 %), their low cost and acceptable lifetime (at least 20 years under operational conditions) have attracted great attention [5]. These solar cells are made of photoanode that is a mesoporous oxide film combined with semiconductor particles at the nanometer-scale. The semiconductor particles that are protected by a transparent conductive oxide are usually  $\text{TiO}_2$ . Dye molecule that is placed on the photoanode, absorbs photon flux emitted from the sun. Also, it can protect the contacting of  $\text{TiO}_2$  surface with the electrolyte solution and consequently prevents from charge recombination process [6]. Afterward the photo-excited electron from dye molecule is injected into the conduction band of semiconductor and through the distribution of electron in it, current is generated. The electron proceeds to the counter electrode that is placed in adjacency of a electrolyte solution. Then redox couple in the solution transfers electron to dye molecule and eventually dye molecule is regenerated to ground state [2, 7].

In this paper, dye sensitized solar cells based on N3

dye molecule (which has been the subject of a combined experimental and theoretical study [8]), with an electrolyte of iodide/triiodide redox couple are investigated. The N3 dye molecule is placed in category of Ruthenium Polypyridyl sensitizer dyes and has 59 atoms including Ru, N, S, C, O and H atoms [7]. The optimized molecular structure of N3 is displayed in Fig. 1. This molecule absorbs incident sunlight photon in a range of visible spectrum, has a high thermal stability and excited states with high lifetime which have led to be recognized as an efficient sensitizer. In addition, the acid carboxylic group (COOH) used to putting dye on the surface of the semiconductor [9]. Redox couple in the electrolyte solution, iodide/triiodide, has an acceptable redox potential, is soluble and accelerates the dye regeneration process. On the other hand, its slow exchange current density on the surface of  $\text{TiO}_2$  leads to reducing unwanted charge recombination on the interface of  $\text{TiO}_2$  and redox couple ('the dark current'). Therefore, due to these characteristics,  $\text{I}^-/\text{I}_3^-$  redox couple is superior than others [10].

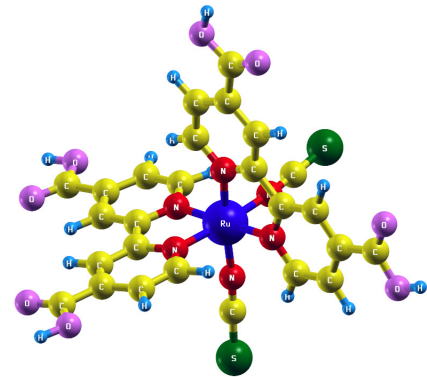
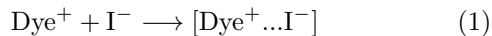


FIG. 1. Optimized structure of N3 dye. The blue, red, yellow, violet, green and light blue spheres represent Ru, N, C, O, S and H atoms, respectively.

In some studies by Clifford et al., dye regeneration process has been suggested through the formation of an unstable intermediate complex according to the following reactions:



This process is accompanied by liberalization of diiodide ( $\text{I}_2^-$ ) [11, 12]. The unstable intermediate complexes  $[\text{Dye}^+ \dots \text{I}^-]$  can be formed in several ways, that depends on the bonding of iodine atom with dye molecule. Here, we have examined two more likely  $[\text{N3}^+ \dots \text{I}^-]$  complexes. In the first one,  $[\text{N3}^+ \dots \text{I}_{\text{Ru}}^-]$ , the iodine atom is located between two pyridine (dcbpy) rings, while bonding of iodine to the hydrogen atom of carboxylic group ( $\text{COOH}$ ) give rises to the second more likely complex,  $[\text{N3}^+ \dots \text{I}_{\text{OH}}^-]$ . For as much as  $[\text{N3}^+ \dots \text{I}^-]$  intermedium is still able to absorption of another iodide ion,  $\text{N3I}_{\text{Ru}} - \text{I}^-$  and  $\text{N3I}_{\text{OH}} - \text{I}^-$  complexes construct, that in them the second  $\text{I}^-$  is interacted with first  $\text{I}^-$  of  $[\text{N3}^+ \dots \text{I}_{\text{Ru}}^-]$  and  $[\text{N3}^+ \dots \text{I}_{\text{OH}}^-]$  respectively [11], [13]. First-principles investigation of the structural, chemical, and energetic properties of these complexes would be helpful for better perception of the dye regeneration process. Moreover, we will also determine the minimum energy path for the proposed reactions.

## II. COMPUTATIONAL DETAILS

Our electronic structure calculations and geometry optimizations have been performed in the framework of density functional theory (DFT) by using PAW pseudopotential as well as numerical orbital - full potential techniques implemented in the Quantum Espresso (QE) [14] and FHI-aims [15] computational packages, respectively. We used GGA-PBE exchange-correlation functional, [16] and supercell approach for simulation of isolated dye molecules in QE. A vacuum thickness of about 20 Bohr was utilized to avoid interaction of adjacent molecules. Energy cutoffs of 30 Ry and 300 Ry, were used for plane wave expansion of wave functions and electron density, while full potential calculations were performed with *tier2* basis set and atomic ZORA scalare relativistic effects.

The optical absorption spectrum of the molecules were calculated in the framework of Liouville-Lanczos approach to time-dependent DFT, implemented in Turbo-TDDFT code [17, 18], that is part of the Quantum Espresso distribution. The Nudged Elastic Band (NEB) method [19], implemented in Quantum Espresso, was also used to determine the reaction path.

## III. RESULTS AND DISCUSSIONS

### A. Structural properties

As already mentioned in dye regeneration mechanism, the N3 dye is excited by absorbing photons, and turns to the  $\text{N3}^+$ . Afterwards, interaction of the  $\text{N3}^+$  with the iodide redox shuttle cause the dye regeneration. By repeating this cycle processes, current is generated. Hence, the oxidized dye ( $\text{N3}^+$ ) plays a crucial role in the mechanisms that occur in the electrolyte. The atomic bond lengths of N3 and its oxidized form,  $\text{N3}^+$ , are shown in Fig. 2. The calculated bond lengths are in agreement with the reported findings by Asaduzzaman et al. [11].

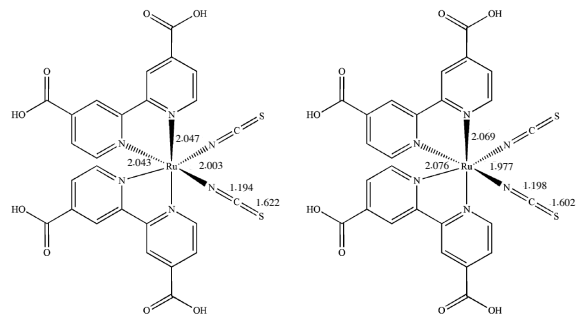


FIG. 2. Schematic representation of the optimized structure of N3 dye and its oxidized form,  $\text{N3}^+$ . The numbers in the figure, show the corresponding bond length in Angstrom.

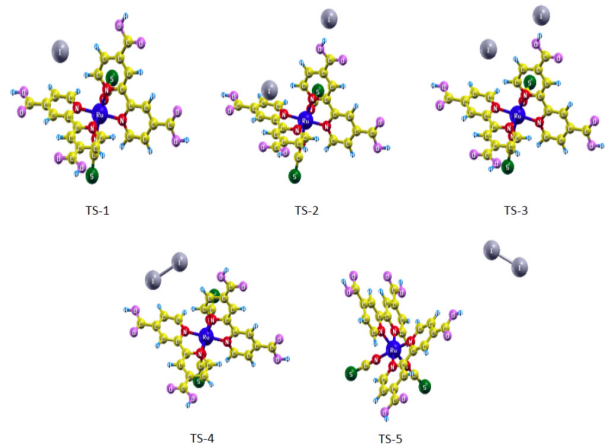


FIG. 3. Optimized structure of transition states. TS - 1 corresponds to  $\text{N3}^+ \text{I}^-$ , and other transition states correspond to  $\text{N3I}_2^-$ . Also TS - 2 and TS - 4 are related to  $[\text{N3}^+ \dots \text{I}_{\text{Ru}}^-]$  while TS - 3 and TS - 5 are related to  $[\text{N3}^+ \dots \text{I}_{\text{OH}}^-]$ .

The values indicate that oxidation of N3 increases the bond length between Ru and Pridine (dcbpy) rings and decreases the bond distance between Ru and NCS groups. Actually, the Ru atom in  $\text{N3}^+$ , compared with N3, has

one less electron for covalent bonding with dcby rings, hence the corresponding bond distance become longer. On the other hand, increasing the charge on Ru atom, enhances and consequently shorten the ionic bonding between Ru and NCS groups.

As previously mentioned,  $I^-$  may interact with the electropositive parts of  $N3^+$  to construct  $[N3^+...I^-]$  complexes. Ru atom has a positive charge in  $N3^+$ , but it has already been occupied with six bonds. So  $I^-$  could not interact with Ru atom and for this reason,  $I^-$  interacts with the dcby rings to form  $[N3^+...I_{Ru}^-]$  complex. Also, there are two options for interaction of the  $I^-$  with H atoms of  $N3^+$ : The  $I^-$  can interact with H atoms, those related to the dcby rings and those related to the carboxylic groups (COOH). For as much as the H atoms that are part of the carboxylic groups, are more electropositive, their interaction with  $I^-$  leads to the formation of the more stable forms of  $[N3^+...I_{OH}^-]$  complex. In the next step, the second iodide ion interacts with the first iodide ion in  $[N3^+...I_{Ru}^-]$  and  $[N3^+...I_{OH}^-]$  complexes, so  $N3I_{Ru} - I^-$  and  $N3I_{OH} - I^-$  complexes are constructed, respectively. Also, it is possible to the second iodide ion interacts with the H atoms of different carboxylic groups (COOH), but the complexes formed in this way are less stable [11]. Therefore, we have not considered these unstable complexes for this article. The stable complexes are formed through the reactions would mention in appendix that depending on the status of iodine in complexes have been examined separately.

Theoretical efforts to achieve the transition states of the formation of  $[N3^+...I_{Ru}^-]$  and  $[N3^+...I_{OH}^-]$  have failed [11]. These efforts only led to finding a transition state that is created during the conversion of  $[N3^+...I_{Ru}^-]$  to  $[N3^+...I_{OH}^-]$ . In other words, iodine has moved from its place in  $[N3^+...I_{Ru}^-]$  to that in  $[N3^+...I_{OH}^-]$  through the transition state that was named  $TS - 1$ . The next transition states are obtained via the mentioned reactions [11]. The optimized structures of transition states are shown in Fig. 3. The Ru - I, H - I and I - I distances of the  $N3^+I^-$  and  $N3I_2^-$  complexes and mentioned transition states are tabulated in table I.

After optimization, the magnetic properties of the system were investigated. For this purpose, using optimized structures and considering an initial moment on iodine, we performed spin-polarized calculations to determine the total magnetization of N3 and its derivatives, listed in table I. It is seen that the N3 dye molecule is non-magnetic while its studied derivatives have a spin moment of  $1 \mu_B$ .

## B. Electronic and Vibrational properties

The electronic structure of the optimized N3 molecule was calculated by using both pseudopotential and full potential techniques and a good agreement was observed. The HOMO-LUMO gap of N3 was found to be 0.64 eV (0.61 eV) within pseudo-potential (full-potential)

method, which is significantly lower than the experimental gap of about 1.67 eV [20]. This difference reflects the main deficiency of LDA/GGA functionals for prediction of the excited states properties. Thereby, in order to achieve reliable results for energy gap, TDDFT calculations will be used.

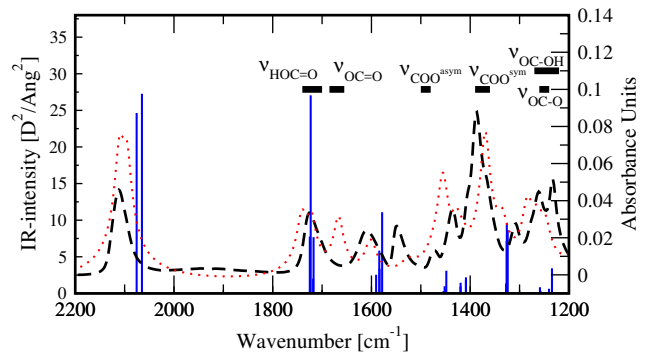


FIG. 4. Blue line: calculated IR spectrum of N3 dye molecule (this work). experimental IR spectrum of N3 adsorbed on anatase nanocrystals in EtOH (black dashed) and the computed IR spectrum (red dotted) for the fully protonated configuration  $I_1$  on the anatase  $TiO_2$  (101) surface [21, 22]).

Orbital density of N3 molecule and some of its derivatives were calculated and displayed in table II. The most activity of electrons are in HOMO state. So we are enthusiastic to investigate the HOMO-LUMO orbitals of each structure. As shown in table II, the orbital density is more in HOMO orbitals than others and there are a lot of active electrons here, that are ready to charge exchange and reactions. This fact confirms the reaction of iodine atom in complexes.

The vibrational spectra of the molecule was calculated to investigate dynamical stability and IR spectrum of the systems. The obtained IR spectrum of the N3 molecule is shown in Fig. 4. Absence of any imaginary mode in the spectrum, confirms dynamical stability of the molecule. As is evident, vibrations around 2100 ( $cm^{-1}$ ) and 1700 ( $cm^{-1}$ ) frequencies have higher IR intensity and they are related to the stronger bonds. For comparison, the computational and experimental infrared spectrum of the N3 molecule adsorbed on  $TiO_2$  anatase, taken from ref. [21], are also displayed in Fig. 4. We observe that the two highest energy peaks of our spectrum, are also visible in the spectrum of the adsorbed molecule, while the lower energy peaks does not match correctly. It may be attributed to the presence of  $TiO_2$  substrate.

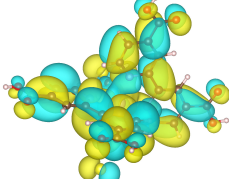
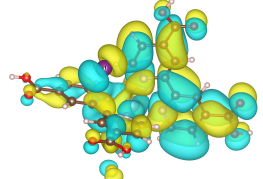
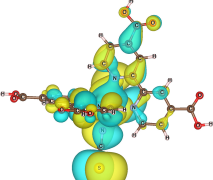
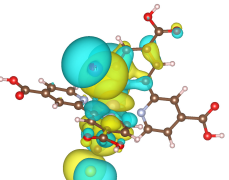
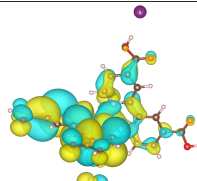
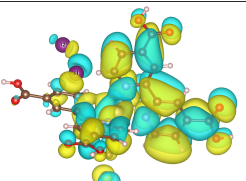
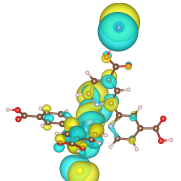
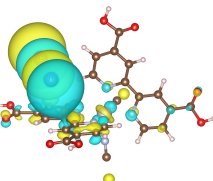
## C. Optical properties

Absorption spectra of dye molecule play a significant role in the efficiency of solar cells, hence first-principles calculation of this property is desired. To determine the optical spectrum, the Liovile-lanzcos approach with TDFT was used. In this approach, an important pa-

TABLE I. Calculated bond lengths ( $\text{\AA}$ ), total magnetization  $\mu$  ( $\mu_B$ ), and optical gap of the N3 molecule and its derivatives. The presented bond lengths in the paranthesis are taken from ref. [11].

	Bond length			$\mu$	gap
	Ru - I	H - I	I - I		
N3	—	—	—	0.0	1.56
$[\text{N3}^+ \dots \text{I}_{\text{Ru}}^-]$	5.237 (5.234)	—	—	1.0	1.67
$[\text{N3}^+ \dots \text{I}_{\text{OH}}^-]$	—	2.370 (2.392)	—	1.0	1.65
$\text{N3I}_{\text{Ru}} - \text{I}^-$	5.639 (5.637)	—	3.193 (3.265)	1.0	1.50
$\text{N3I}_{\text{OH}} - \text{I}^-$	—	2.394 (2.462)	8.954 (3.062)	1.0	2.24
$TS - 1$	6.193 (8.500)	6.404 (4.043)	—	1.0	1.62
$TS - 2$	5.429 (6.031)	—	8.299 (5.000)	1.0	1.73
$TS - 3$	—	2.350 (2.432)	5.838 (5.500)	1.0	1.65
$TS - 4$	8.183 (8.200)	—	2.940 (3.015)	1.0	1.78
$TS - 5$	—	5.992 (6.000)	17.25 (2.935)	1.0	1.66

TABLE II. Orbital density of N3 dye molecule and its derivatives;  $[\text{N3}^+ \dots \text{I}_{\text{Ru}}^-]$ ,  $[\text{N3}^+ \dots \text{I}_{\text{OH}}^-]$  and  $[\text{N3I}_{\text{Ru}} - \text{I}]$ ; in HOMO and LUMO states.

Phase	a) N3	b) $[\text{N3}^+ \dots \text{I}_{\text{Ru}}^-]$
LUMO		
HUMO		
Phase	c) $[\text{N3}^+ \dots \text{I}_{\text{OH}}^-]$	d) $[\text{N3I}_{\text{Ru}} - \text{I}]$
LUMO		
HUMO		

parameter is number of iterations which should be optimized. We have calculated the absorption spectrum of N3 at different number of iterations (Fig. 5). It is seen that the optical spectrum with 500 iteration is flat while sharp peaks appear by increasing iterations. The obtained absorption spectra with 1500 and 2000 iterations are completely overlapping. Therefore, 1500 iterations is

the optimized parameter for our subsequent calculations.

The optical spectrum of N3 molecule, its complexes, and the transition states are shown in Fig. 6. The first peak in the absorption spectrum represents the first excited state and its energy is equal to the required energy for the transition of an electron from the highest occupied molecular orbital (HOMO) to the lowest unoccu-

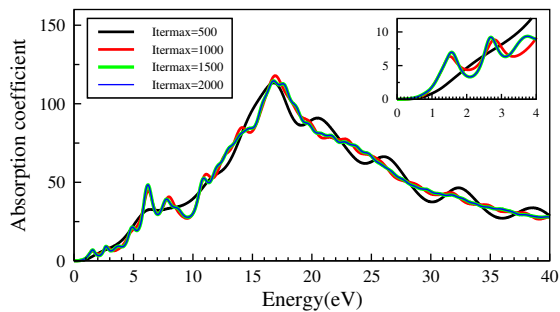


FIG. 5. Optimizing the number of iterations to determine the optical spectrum of the N3 dye molecule.

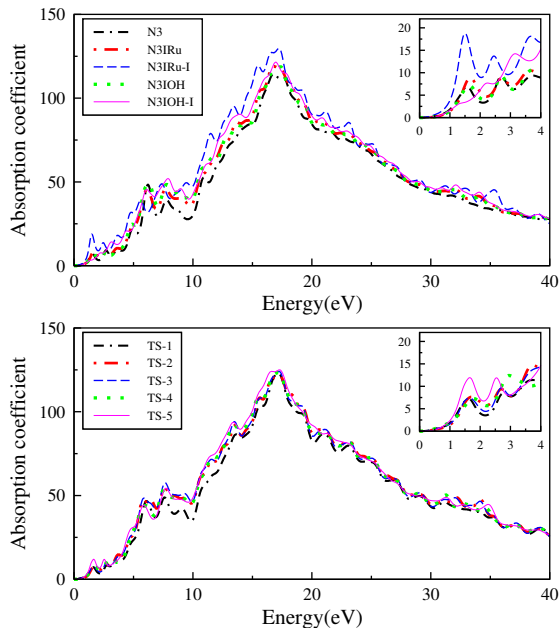


FIG. 6. Obtained absorption optical spectrum of N3, its complexes, and corresponding transition states. The insets show the initial part of the spectra in a narrow window.

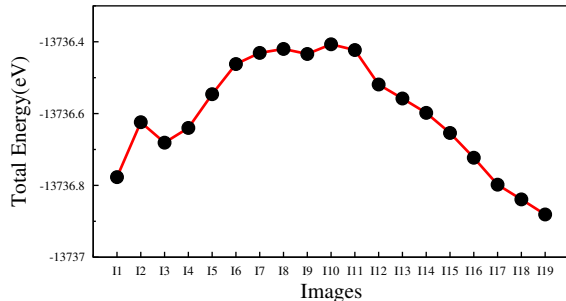


FIG. 7. Obtained minimum energy path for reaction 3, The 10th image is considered as the transition state where I1 stands for  $[N3^+ \dots I_{Ru}^-]$  and I19 for  $[N3^+ \dots I_{OH}^-]$ .

pied molecular orbital (LUMO), which is indeed representative of the optical gap. The next peaks in the absorption spectrum show the next excitation of electrons

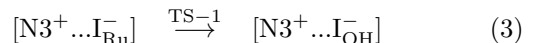
from other states. By increasing the energy difference between states, excitation occurs in higher energy. The first peak is only related to one excitation (first excitation), while the next peaks are related to some excitations which broadening of each peak depends on the number of electron excitations in the corresponding energy. The optical gap is calculated for structures and the results are listed in table I. The optical gap of N3 molecule is compared with its experimental gap and the conformity of them is perfectly clear.

TABLE III. The required activation energy for the reactants in which transition states is formed.

structure	$E_a(NEB)$	$E_a(Quantum - Espresso)$	$E_a ([11])$
TS - 1	8.52	5.68	7.33
TS - 2	-	-	4.18
TS - 3	-	-	9.57
TS - 4	-	4.18	5.33
TS - 5	-	3.44	5.20

#### D. Reaction path

As previously mentioned, the dye regeneration mechanism happens through the formation of intermediate complexes and transition states. Since determination of lowest energy path is the one of the most important issue which we are dealing with, it can be useful to calculate it with Nudged Elastic Band (NEB) method. By using NEB method, it is possible to determine Minimum Energy Path (MEP), saddle point energy (maximum potential energy along the MEP), activation energy barrier, estimated transition rate and also configuration of atoms during the transition. Minimum Energy Path is calculated for reaction which states in eq. 3 by considering 19 images. In this method, a path with the lowest energy is determined for the reaction then a string of images of the system are created. In fact, images of the system are the intermediate configurations of system. Finally, the images are connected together through the hypothetical springs with the same spring constant [23], [24]. The representation of reaction path, from the reactant configuration to the product configuration, is formed.  $[N3^+ \dots I_{Ru}^-]$  and  $[N3^+ \dots I_{OH}^-]$  complexes are considered as the initial and final images, respectively and remain constant during the run. Also, intermediate images are obtained by using interpolation. It results an energy for each images. Minimum Energy Path, obtained from NEB method, is displayed in Fig. 7.



It can be seen from Fig. 7 that  $[N3^+ \dots I_{Ru}^-]$  complex has a higher energy level than  $[N3^+ \dots I_{OH}^-]$  complex, so

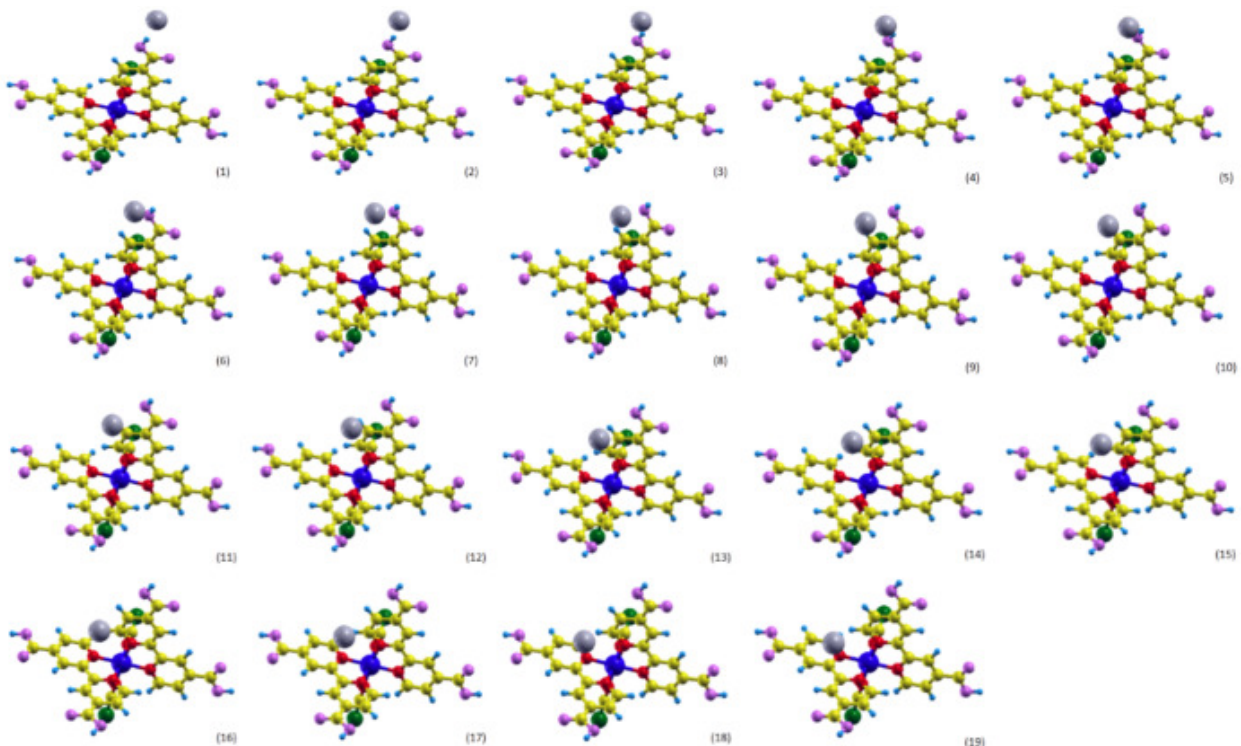


FIG. 8. configuration formed during the path of reaction 3. The first structure is  $[N3^+ \dots I_{Ru}^-]$ , the last structure is  $[N3^+ \dots I_{OH}^-]$ , and the 10th structure is TS-1.

$[N3^+ \dots I_{OH}^-]$  complex is more stable than  $[N3^+ \dots I_{Ru}^-]$  complex and the occurrence of reaction is possible. Also, the second image has higher energy than its adjacent images. This increase in energy indicating weak bond formed during the reaction path, which is not unexpected. Moreover, tenth image has a maximum energy among other images and we introduce it as the transition state of reaction. The activation energy obtained by this method is presented in Table III and is compared with the activation energy obtained from other calculations. By comparing the values presented in Table III, we can see that the activation energy obtained from Nudged Elastic Band method has a better accordance with the activation energy reported in other studies, hence it can be said that the NEB method is a good and reliable method to determine the reaction path.

Since in another reactions, the two reactants are converted to one product, calculation of the activation energy is not possible by using NEB method. In this case there are infinite situations for the location of the two reactants towards each other which is impossible to consider all situations, hence NEB method was used just for a reaction in which TS-1 transition state is formed.

As previously mentioned, one of the advantages of NEB method is determination of the configuration of atoms in any part of the reaction path. Due to the number of images that we have considered, 19 configuration is determined using interpolation. These configurations are displayed in Fig. 8. As we know, TS-1 structure is a tran-

sition state that is achieved from conversion of  $[N3^+ \dots I_{Ru}^-]$  to  $[N3^+ \dots I_{OH}^-]$ . Also it can be seen clearly from Fig. 8 that iodine has moved from its place in  $[N3^+ \dots I_{Ru}^-]$  to that in  $[N3^+ \dots I_{OH}^-]$ .

#### IV. CONCLUSION

Density functional calculations were performed to investigate the structural, electronic, vibrational and optical properties of N3 dye molecule, using both Quantum Espresso and FHI-aims Computational packages. We found that complexes of N3 and transition states have magnetic properties. The obtained results from calculated IR spectrum indicate that N3 dye molecule is a stable structure. Also, we have chosen the most stable of  $[dye^+ \dots I^-]$  complexes for our calculations. We calculated optical gap of N3 dye molecule using optical spectrum, then compared with experimental gap. The conformity of optical gap and experimental gap demonstrate the success of Liouville-Lanczos approach in calculating the optical gap and determination of optical gap. Also, we determine the minimum energy path of reaction 3 and its activation energy, using Nudged Elastic Band method. It was discussed that the tenth image is TS-1. In summery, investigation of details about mechanism of interactions between  $I/I_3^-$  and N3 dye molecule can help us to a better understanding of dye regeneration and provide factors for

raising efficiency or in the other words, it could be paving the way to achieve higher efficiency.

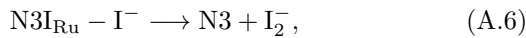
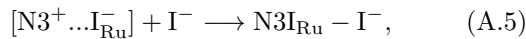
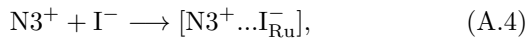
## V. ACKNOWLEDGMENTS

We would like to acknowledge the Isfahan University of Technology. The authors gratefully acknowledge the Sheikh Bahaei National High Performance Computing Center (SBNHPCC) for providing computing facilities and time. SBNHPCC is supported by scientific and technological department of presidential office and Isfahan University of Technology (IUT).

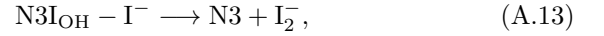
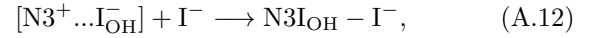
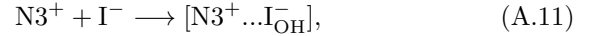
### Appendix: Photovoltaic mechanism

The stable complexes formed through the following reactions, depends on the status of iodine in the complexes.

1. Reactions involving the formation of complexes  $[\text{N3}^+ \dots \text{I}_{\text{Ru}}^-]$  and  $\text{N3I}_{\text{Ru}} - \text{I}^-$ :

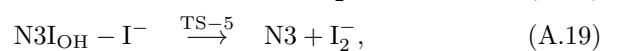
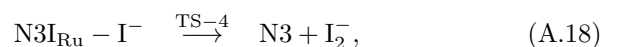
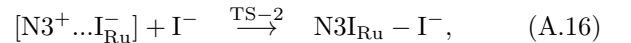
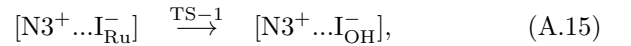


2. Reactions involving the formation of complexes  $[\text{N3}^+ \dots \text{I}_{\text{OH}}^-]$  and  $\text{N3I}_{\text{OH}} - \text{I}^-$ :



The optimized structures of  $\text{N3}^+\text{I}^-$  ( $[\text{N3}^+ \dots \text{I}_{\text{Ru}}^-]$ ,  $[\text{N3}^+ \dots \text{I}_{\text{OH}}^-]$ ) and  $\text{N3I}_2^-$  ( $\text{N3I}_{\text{Ru}} - \text{I}^-$ ,  $\text{N3I}_{\text{OH}} - \text{I}^-$ ) complexes are shown in Fig. 9.

During this reactions, the five transition states will be formed which are as follows:



- 
- [1] N. Panwar, S. Kaushik, and S. Kothari, *Renewable and Sustainable Energy Reviews* **15**, 1513 (2011).
  - [2] A. M. Bagher, M. Mahmoud, A. Vahid, and M. Mohsen, *American Journal of Optics and Photonics* **3(5)**, 94 (2015).
  - [3] M. Green and K. Emery, *Progress in ...* **22**, 701 (2015).
  - [4] G. W. Crabtree and N. S. Lewis, *Physics today* **60**, 37 (2007).
  - [5] M. Grätzel, *Comptes Rendus Chimie* **9**, 578 (2006).
  - [6] M. Pastore, E. Mosconi, and F. De Angelis, *The Journal of Physical Chemistry C* **116**, 5965 (2012).
  - [7] Grätzel, M., *Journal of Photochemistry and Photobiology C: Photochemistry Reviews* **4**, 145 (2003).
  - [8] G. Pizzoli, M. G. Lobello, B. Carlotti, F. Elisei, M. K. Nazeeruddin, G. Vitillaro, and F. De Angelis, *Dalton Transactions* **41**, 11841 (2012).
  - [9] F. De Angelis, S. Fantacci, and A. Selloni, *Chemical physics letters* **389**, 204 (2004).
  - [10] G. Boschloo and A. Hagfeldt, *Accounts of Chemical Research* **42**, 1819 (2009).
  - [11] A. Asaduzzaman and G. Schreckenbach, *Physical Chemistry Chemical ...* **13**, 15148 (2011).
  - [12] J. N. Clifford, E. Palomares, M. K. Nazeeruddin, M. Grätzel, and J. R. Durrant, *The Journal of Physical Chemistry C* **111**, 6561 (2007).
  - [13] M. Xie, J. Chen, F.-Q. Bai, W. Wei, and H.-X. Zhang, *The Journal of Physical Chemistry A* **118**, 2244 (2014).
  - [14] P. Giannozzi, S. Baroni, N. Bonini, M. Calandra, R. Car, C. Cavazzoni, D. Ceresoli, G. L. Chiarotti, M. Cococcioni, I. Dabo, A. Dal Corso, S. de Gironcoli, S. Fabris, G. Fratesi, R. Gebauer, U. Gerstmann, C. Gougoussis, A. Kokalj, M. Lazzeri, L. Martin-Samos, N. Marzari, F. Mauri, R. Mazzarello, S. Paolini, A. Pasquarello, L. Paulatto, C. Sbraccia, S. Scandolo, G. Sclauzero, A. P. Seitsonen, A. Smogunov, P. Umari, and R. M. Wentzcovitch, *Journal of physics. Condensed matter* **21**, 395502 (2009).
  - [15] V. Blum, R. Gehrke, F. Hanke, and P. Havu, *Computer Physics ...* **1** (2009).
  - [16] J. P. Perdew, K. Burke, and M. Ernzerhof, *Phys. Rev. Lett.* **77**, 3865 (1996).
  - [17] O. B. Malcıoğlu, R. Gebauer, D. Rocca, and S. Baroni, *Computer Physics Communications* **182**, 1744 (2011).
  - [18] C. A. Ullrich and Z.-h. Yang, *Brazilian Journal of Physics* **44**, 154 (2014).
  - [19] K. Caspersen and E. Carter, *Proceedings of the National Academy of Sciences of the United States of America* **102**, 6738 (2005), cited By 31.

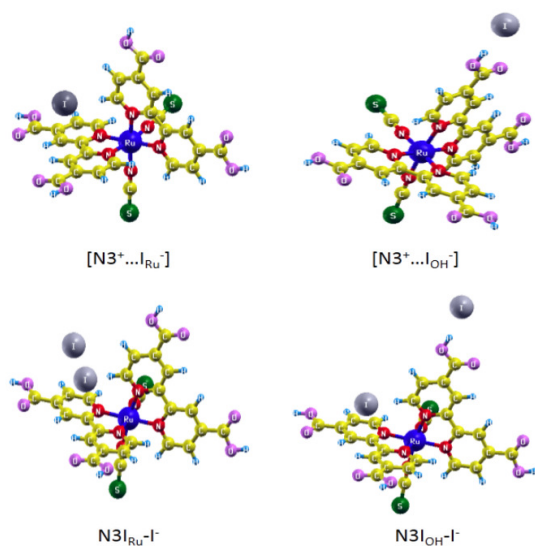


FIG. 9. Optimized structure of  $N3^+I^-$  ( $[N3^+ \dots I_{Ru}^-]$ ,  $[N3^+ \dots I_{OH}^-]$ ) and  $N3I_2^-$  ( $N3I_{Ru}^- I^-$ ,  $N3I_{OH}^- I^-$ ) complexes.

- [20] E. Bersch and S. Rangan, *APS Meeting ...* **1**, 36006 (2008).
- [21] Y. Bai, I. Mora-Seró, F. De Angelis, J. Bisquert, and P. Wang, *Chemical reviews* **114**, 10095 (2014).
- [22] F. Schiffmann, J. VandeVondele, J. Hutter, R. Wirz, A. Urakawa, and A. Baiker, .
- [23] G. Mills and K. W. Jacobsen, in *In Classical and quantum dynamics in condensed phase simulations* (University of Washington, 1998) pp. 385–404.
- [24] H. Henkelman, G., Johannesson, G. and Jonsson, in *in Theoretical Methods in Condensed Phase Chemistry* (2002) pp. 269–300.